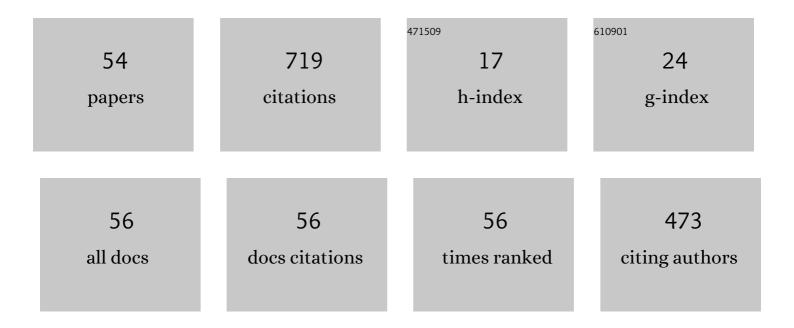
Bo Song

List of Publications by Year in descending order

Source: https://exaly.com/author-pdf/4794193/publications.pdf Version: 2024-02-01



RO SONC

#	Article	IF	CITATIONS
1	Effect of Mg, La and Ca addition order on inclusions and microstructure of Ti-bearing C–Mn steel. Ironmaking and Steelmaking, 2022, 49, 189-198.	2.1	2
2	Designing cross-region ecological compensation scheme by integrating habitat maintenance services production and consumption—A case study of Jing-Jin-Ji region. Journal of Environmental Management, 2022, 311, 114820.	7.8	7
3	Effect of Al and S on the Evolution of Inclusion and Formation of Acicular Ferrite in the Mg-RE-Ti-Treated Steel. Transactions of the Indian Institute of Metals, 2022, 75, 2221-2230.	1.5	2
4	Directional separation of nonmetallic inclusions from copper melt reinforced by supergravity. Metallurgical Research and Technology, 2022, 119, 307.	0.7	0
5	Effect of Rare Earth Ce on Modifying Inclusions in Al-killed X80 Pipeline Steel. Transactions of the Indian Institute of Metals, 2022, 75, 2837-2846.	1.5	6
6	A Mathematical Model of COREX Process with Top Gas Recycling. Steel Research International, 2021, 92, 2000292.	1.8	6
7	Evolution of inclusions in Mg-RE-Ti treated steels with different Al contents and their influence on acicular ferrite. Metallurgical Research and Technology, 2021, 118, 208.	0.7	3
8	Influence of top gas recycling technology on operation parameters and CO2 emission of COREX process. Ironmaking and Steelmaking, 2021, 48, 693-702.	2.1	2
9	Effect of Ca on the evolution of inclusions and the formation of acicular ferrite in Ti–Mg killed EH36 steel. Ironmaking and Steelmaking, 2021, 48, 1115-1122.	2.1	3
10	Effects of Mg and La on the evolution of inclusions and microstructure in Ca-Ti treated steel. International Journal of Minerals, Metallurgy and Materials, 2021, 28, 1940-1948.	4.9	19
11	Influence of temperature on the microstructure and physical properties of corundum refractory brick in the blast furnace hearth. Ironmaking and Steelmaking, 2020, 47, 263-270.	2.1	3
12	Effects of finish rolling deformation on hydrogen-induced cracking and hydrogen-induced ductility loss of high-vanadium TMCP X80 pipeline steel. International Journal of Hydrogen Energy, 2020, 45, 30828-30844.	7.1	10
13	Effect of Tempering Temperature after Thermo-Mechanical Control Process on Microstructure Characteristics and Hydrogen-Induced Ductility Loss in High-Vanadium X80 Pipeline Steel. Materials, 2020, 13, 2839.	2.9	7
14	Effect of Cerium Content on the Evolution of Inclusions and Formation of Acicular Ferrite in Ti-Mg-Killed EH36 Steel. Metals, 2020, 10, 863.	2.3	12
15	Microstructure and physical properties of a mullite brick in blast furnace hearth: influence of temperature. Ironmaking and Steelmaking, 2020, , 1-7.	2.1	4
16	The Interaction Force between Scheelite and Scheelite/Fluorite/Calcite Measured Using Atomic Force Microscopy. Journal of Chemistry, 2020, 2020, 1-15.	1.9	1
17	Effect of Mg on the Evolution of Inclusions and Formation of Acicular Ferrite in La–Tiâ€Treated Steels. Steel Research International, 2020, 91, 1900563.	1.8	19
18	Effects of CeO ₂ on Melting Temperature, Viscosity, and Structure of CaF ₂ -bearing and B ₂ O ₃ -containing Mold Fluxes for Casting Rare Earth Alloy Heavy Rail Steels. ISIJ International, 2019, 59, 1242-1249.	1.4	11

Bo Song

#	Article	IF	CITATIONS
19	Effect of CeO2 on heat transfer and crystallization behavior of rare earth alloy steel mold fluxes. International Journal of Minerals, Metallurgy and Materials, 2019, 26, 565-572.	4.9	8
20	Influence of Tempering Treatment on Precipitation Behavior, Microstructure, Dislocation Density and Hydrogen-Induced Ductility Loss in High-Vanadium Hot-Rolled X80 Pipeline Steel. Minerals, Metals and Materials Series, 2019, , 1111-1122.	0.4	1
21	Effect of Vanadium and Titanium on Desulfurization of CaO Slag in Liquid Iron. Metals, 2019, 9, 1239.	2.3	1
22	Effect of vanadium content on hydrogen diffusion behaviors and hydrogen induced ductility loss of X80 pipeline steel. Materials Science & Engineering A: Structural Materials: Properties, Microstructure and Processing, 2019, 742, 712-721.	5.6	40
23	The Microstructure and Property of the Heat Affected zone in C-Mn Steel Treated by Rare Earth. High Temperature Materials and Processes, 2019, 38, 362-369.	1.4	6
24	Reliability analysis of wind turbines under nonâ€Gaussian wind load. Structural Design of Tall and Special Buildings, 2018, 27, e1443.	1.9	4
25	Effects of cooling processes on microstructure and susceptibility of hydrogenâ€induced cracking of X80 pipeline steel. Materials and Corrosion - Werkstoffe Und Korrosion, 2018, 69, 590-600.	1.5	5
26	Separation of Non-metallic Inclusions from a Fe-Al-O Melt Using a Super-Gravity Field. Metallurgical and Materials Transactions B: Process Metallurgy and Materials Processing Science, 2018, 49, 34-44.	2.1	6
27	Macrosegregation behavior of solute Cu in the solidifying Al-Cu alloys in super-gravity field. Metallurgical Research and Technology, 2018, 115, 506.	0.7	6
28	Synthesis and densification of zirconium diboride prepared by carbothermal reduction. Rare Metals, 2018, 37, 1076-1081.	7.1	7
29	Multi-Objective Optimization of Cost Saving and Emission Reduction in Blast Furnace Ironmaking Process. Metals, 2018, 8, 979.	2.3	5
30	Effect of heat input on microstructure and toughness of rare earth-contained C–Mn steel. Journal of Iron and Steel Research International, 2018, 25, 1033-1042.	2.8	9
31	Effects of vanadium precipitates on hydrogen trapping efficiency and hydrogen induced cracking resistance in X80 pipeline steel. International Journal of Hydrogen Energy, 2018, 43, 17353-17363.	7.1	58
32	Effect of Super-gravity Field on Grain Refinement and Tensile Properties of Cu–Sn Alloys. ISIJ International, 2018, 58, 98-106.	1.4	22
33	Effect of Ti–Mg Treatment on the Impact Toughness of Heat Affected Zone in 0.15%C–1.31%Mn Steel. Steel Research International, 2018, 89, 1700355.	1.8	16
34	Effects of Mn and Al on the Intragranular Acicular Ferrite Formation in Rare Earth Treated C–Mn Steel. High Temperature Materials and Processes, 2017, 36, 683-691.	1.4	7
35	Role of Lanthanum Addition on Acicular Ferrite Transformation in C–Mn Steel. ISIJ International, 2017, 57, 1261-1267.	1.4	38
36	Effect of Super Gravity on the Solidification Structure and C Segregation of High-Carbon Steel. Minerals, Metals and Materials Series, 2017, , 571-579.	0.4	0

Bo Song

#	Article	IF	CITATIONS
37	The Refining Mechanism of Super Gravity on the Solidification Structure of Al-Cu Alloys. Materials, 2016, 9, 1001.	2.9	30
38	Removal of Inclusions from Molten Aluminum by Supergravity Filtration. Metallurgical and Materials Transactions B: Process Metallurgy and Materials Processing Science, 2016, 47, 3435-3445.	2.1	21
39	Enriching and Separating Primary Copper Impurity from Pb-3 Mass Pct Cu Melt by Super-Gravity Technology. Metallurgical and Materials Transactions B: Process Metallurgy and Materials Processing Science, 2016, 47, 2714-2724.	2.1	22
40	Electrochemical reduction behavior of Hf(IV) in molten NaCl–KCl–K2HfCl6 system. Rare Metals, 2016, 35, 655-660.	7.1	5
41	Effect of Arsenic and Copper+Arsenic on High Temperature Oxidation and Hot Shortness Behavior of C–Mn Steel. ISIJ International, 2016, 56, 1232-1240.	1.4	14
42	Effect of arsenic content and quenching temperature on solidification microstructure and arsenic distribution in iron-arsenic alloys. International Journal of Minerals, Metallurgy and Materials, 2015, 22, 704-713.	4.9	11
43	Separating Behavior of Nonmetallic Inclusions in Molten Aluminum Under Super-Gravity Field. Metallurgical and Materials Transactions B: Process Metallurgy and Materials Processing Science, 2015, 46, 2190-2197.	2.1	34
44	Effect of Cerium on Characteristic of Inclusions and Grain Boundary Segregation of Arsenic in Iron Melts. Steel Research International, 2015, 86, 1430-1438.	1.8	29
45	Formation of Acicular Ferrite in Mg Treated Ti-bearing C–Mn Steel. ISIJ International, 2015, 55, 1468-1473.	1.4	32
46	Effect of Manganese Sulphide Size on the Precipitation of Tin Heterogeneous Nucleation in as-Cast Steel. High Temperature Materials and Processes, 2015, 34, .	1.4	1
47	Dielectric properties and energy-storage performances of (1Ââ ^{~,} Âx)Pb(Mg1/3Nb2/3)O3–xPbTiO3 relaxor ferroelectric thin films. Journal of Materials Science: Materials in Electronics, 2015, 26, 9583-9590.	2.2	27
48	Effect of manganese sulfide on the precipitation behavior of tin in steel. International Journal of Minerals, Metallurgy and Materials, 2014, 21, 654-659.	4.9	7
49	In Situ Observation of the Evolution of Intragranular Acicular Ferrite at Mg-containing Inclusions in 16Mn Steel. Journal for Manufacturing Science and Production, 2013, 13, .	0.1	1
50	Large enhancement of energy-storage properties of compositional graded (Pb1â^'xLax)(Zr0.65Ti0.35)O3 relaxor ferroelectric thick films. Applied Physics Letters, 2013, 103, .	3.3	46
51	Influence of Ce on Characteristics of Inclusions and Microstructure of Pure Iron. Journal of Iron and Steel Research International, 2011, 18, 38-44.	2.8	22
52	Effect of austenitizing temperature on microstructure in 16Mn steel treated by cerium. International Journal of Minerals, Metallurgy and Materials, 2011, 18, 652-658.	4.9	18
53	Intragranular Ferrite Formation Mechanism and Mechanical Properties of Non-quenched-and-tempered Medium Carbon Steels. Steel Research International, 2008, 79, 390-395.	1.8	41
54	Evolution of Inclusions and Microstructure in Ca‣aâ€Treated Câ€Mn Steel with Different Mg Contents. Steel Research International, 0, , 2200319.	1.8	1